Conf-940854--2

LA-UR- 94-3166

Title: ASPECTS OF SURFACE GENERATION IN ORTHOGONAL ULTRAPRECISION MACHINING

Author(s): D. A. Lucca, Oklahoma State University

Y. W. Seo, Oklahoma State University

R. L. Rhorer, LANL, ESA-13

Submitted to: International Production Engineering Research Institute (CIRP)
General Assembly, Singapore
August 21-27, 1994

MASTER

Los Alamos
NATIONAL LABORATORY

Aspects of Surface Generation in Orthogonal Ultraprecision Machining

D. A. Lucca, Y. W. Seo, School of Mechanical and Aerospace Engineering, Oklahoma State University, Stillwater, OK 74078; R. L. Rhorer, Los Alamos National Laboratory, Los Alamos, NM 87545; USA – Submitted by R. R. Donaldson (1)
Received on January 14, 1994

SUMMARY

The depth of the plastically deformed layer at the workpiece surface which resulted in the orthogonal ultraprecision machining of Cu over the range of uncut chip thicknesses of 0.01-10 μm was investigated. Two tools with the same nominal geometry but with differing edge geometries were used to machine both Te-Cu and fine grain Cu . Tool edge geometries were characterized by atomic force microscopy, taking into account the AFM cantilever tip radius. Magnitudes of the measured depths appear to be consistent with values reported in the literature and those arrived at by simple analyses.

Keywords: cutting, surfaces, ultra-precision machining

1. INTRODUCTION

Further development of our understanding of the effects which govern the ultraprecision machining process continues to be driven by the desire to create surfaces of exceptional accuracy and quality. The generation of the surface and near surface structures when components are manufactured has been an extremely important and long standing research issue in cutting (Nakayama and Tamura, 1968; von Turkovich, 1972), grinding (Hahn, 1963) and mechanical working (Dautzenberg et al., 1989). This effect is thought to be particularly important when attempting to generate ultraprecision machined surfaces, and several studies which address the damaged layer resulting from three-dimensional diamond turning have been recently reported (Sugano et al., 1987; Horio et al., 1992; Carr et al., 1991; Evans et al., 1987).

Previous tribological studies have contributed to a fundamental understanding of subsurface flow in sliding systems. In particular, the works of Samuels (Samuels, 1971; Turley and Samuels, 1981), Rigney and Hirth (1979) and the extensive studies of Suh (1986) provide a basis for developing an understanding of the effects of subsurface plastic deformation at sliding interfaces.

Here, we present results of an experimental study of the depth of the plastically deformed layer which results in the orthogonal ultraprecision machining of copper.

2. TOOL EDGE CHARACTERIZATION

Measurement of diamond tool edge geometry is essential for quantitative study of the ultraprecision machining process. Recently reported work has shown significant differences in the forces which result when machining with new and worn single crystal diamond tools of the same nominal geometry at uncut chip thicknesses below several micrometers (Lucca and Seo, 1993a). Subtle differences in edge geometry appear to have a major effect on the resulting forces. However, as a result of the edge sharpness of diamond tools (radii of several hundred nanometers down to tens of nanometers), characterization of the edge geometry has presented a formidable task. Recent studies (Asai et al., 1990; Horio et al., 1992) report on the use of a specially configured SEM with two detectors for quantitative evaluation of diamond tool edge profiles. The use of atomic force microscopy, whereby a diamond tool is positioned directly under the scanning cantilever tip has also shown promise for characterization of single crystal diamond tools (Lucca and Seo, 1993a). Suppliers of commercially available Si_3N_4 cantilevers estimate tip radii to be in the range of 20-40 nm. As a result, when using the force microscope to measure the edge of a diamond tool, there will be a convolution of cantilever tip and tool edge geometries which will become important when the tool edge radius is of the order of the cantilever tip radius. In addition, blunted or non-uniformly etched tips may give unrealistically large measures of the diamond tool edge geometry.

In the present study, a direct measurement of the force microscope cantilever tip radius was made and compensated for in the tool edge geometry obtained by the AFM. Commercially available carboxylate microspheres with a diameter of 519 nm and standard deviation of 7 nm were used for the cantilever tip radius measurements. The microspheres come from their manufacturer as a dilute solution with distilled water. A droplet of the solution was placed on a glass slide which had been cleaned with a solution of 70% methanol/30% ethanol and blown off with ultra-pure air, and allowed to dry for several hours. After drying, the microspheres arrange in an ordered crystalline form, and were scanned with the cantilever tip which was used in the measurements of the tool edge profile. Fig. 1 shows a 3 μm x 3 μm scanned image of the microspheres. The scanning rate was 2 Hz, and the applied force was 10^{-7}-10^{-8} N. To obtain a measure of the cantilever tip radius, circles were fit to the cross-sections of 5 spheres over the valid arc, and an average taken to arrive at an estimate of the tip radius (Fig. 2). The asymmetry seen in Fig. 2 is due, in part, to the fact that the AFM is configured such that the cantilever is inclined at a 10 degree angle to the scan direction. In addition, cantilever tip deflections can also contribute to the tip not being normal to the scan direction, and hence care was taken to minimize the applied cantilever force. Figs. 1 and 2 are the data for the cantilever used to characterize the tools in the present study. From the best-fit circle to the microsphere cross-sections, the microsphere diameter was found to be 590 nm ±10 nm. The actual diameter of 519 nm then implied an estimated cantilever tip radius of 35 nm ±5 nm. In our work, we have used cantilevers with tip radii from 20-40 nm. The cantilevers have a

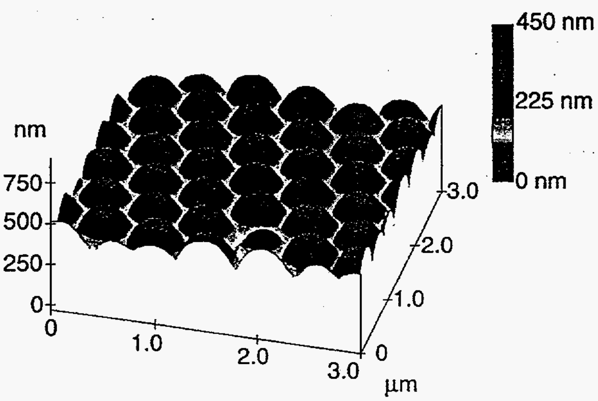

Fig. 1 AFM Scanned Image of 519 nm Diameter Carboxylate Microspheres on a Glass Slide

70 degree pyramidal tip and therefore 110 degrees of usable arc on the tip radius. The maximum arc used for the diamond tool characterization was 95 degrees. The close-packed arrangement of the 519 nm diameter microspheres still allowed for the complete 110 degrees of usable cantilever tip arc to be mapped. After the cantilever tip radius was characterized, 2 mm wide, flat-nosed single crystal diamond tools to be used in the cutting experiments were cleaned and then scanned according to the procedure previously reported (Lucca and Seo, 1993a). After scanning of the diamond tools, the cantilever tip radius was again measured to assure that any changes to its geometry fell within the reported variability of the initial measurement.

3. CUTTING EXPERIMENTS

Orthogonal flycutting experiments were performed on a commercial diamond turning machine by rotating a flat nose, single crystal diamond tool 76.2 mm off the spindle axis to provide the cutting motion. A rectangular workpiece (1 mm wide, 15 mm long) was fixed on top of a piezoelectric dynamometer to allow for the measure of cutting and

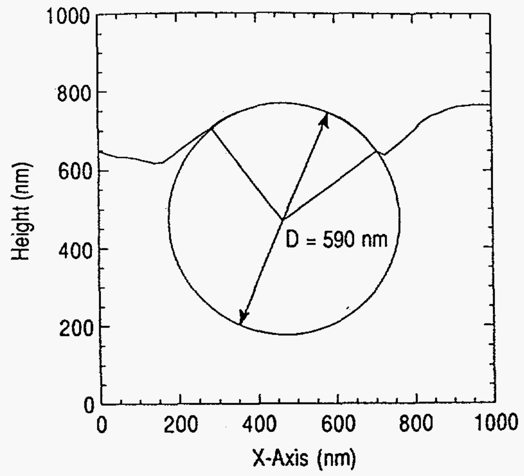

Fig. 2 Cross-Section of AFM Scanned 519 nm Carboxylate Microspheres with Best Fit Circle

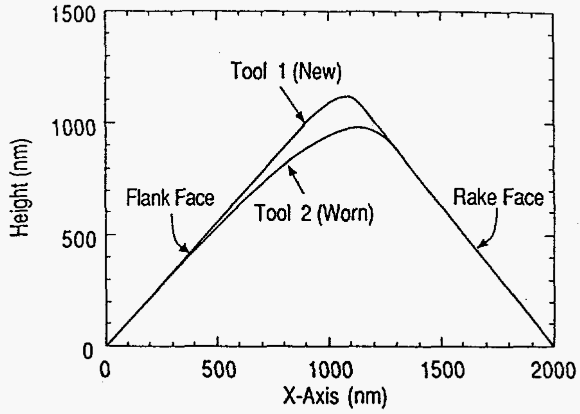

Fig. 3 Measured Edge Profiles of New and Worn Tools After Cantilever Tip Radius Compensation

thrust forces. The workpiece was positioned with its length tangent to the tool motion, also 76.2 mm off axis. The rotating tool's constant infeed rate corresponded to the uncut chip thickness. The magnitude of the off axis dimension compared to the length and width of the workpiece allowed for orthogonal "planing" of the workpiece to be achieved. This configuration is the same as that previously reported (Lucca and Seo, 1993a). The experiments were performed with two workpiece materials, viz., Te-Cu having a nominal chemical composition of 99.4-99.5% Cu and 0.5-0.6% Te and a grain size ranging from about 10-100 µm, and electrolytically deposited pure Cu with a grain size measured to be 4-5 µm. The cutting speed for all the experiments was 47.9 m/min and the uncut chip thickness ranged from 10 µm down to 10 nm. A thin film of heavy mineral oil was brushed onto the workpiece before each cutting test to eliminate intermittent seizing of the tool and workpiece.

The metallographic technique of taper sectioning, employed extensively by Samuels (1971), was used to examine the depth of the plastically deformed layer of the diamond-cut surface. Transverse taper sections were prepared by mounting the 1 x 15 x 12 mm specimens in plastic and then polishing at an acute angle to the diamond-cut surface thus providing a geometric magnification of distances normal to the machined surface. The taper surfaces were prepared by successively polishing the specimen with 240 and 600 grit water-cooled SiC abrasive paper, and then in water slurries of 5 µm, 0.3 µm and 0.05 µm alumina on felt pads. Edge retention in this technique is critical insofar as that the geometry of the taper interface must be known if an accurate estimate of the depth of the subsurface plastically deformed thickness is to be made. A variety of methods to maintain the taper edge have been used, including plating the surface of interest. In the present study the approach was to generate a taper at a nominal acute angle with the diamond-cut surface, and then measure the interface geometry with the laser interferometric microscope. In this way, an accurate measure of the edge geometry as a function of distance away from the taper interface could be used to calculate a subsurface depth. The specimens were then etched by swabbing for 9-20 seconds with a solution of $Fe(NO_3)_3 \cdot 9H_2O$ and HCl to reveal the plastically deformed layer.

4. RESULTS AND DISCUSSION

Using the orthogonal cutting geometry, the depth of subsurface plastic deformation for a given uncut chip thickness, and resulting cutting and thrust force was determined. Uncut chip thickness was varied three orders of magnitude from 10 µm down to 10 nm. These effects were investigated for new and worn tools for both Te-Cu and fine grain pure Cu. The tools were each characterized under an optical microscope as having a nominal geometry of 0 degree rake angle, and 5 degree clearance angle. The edge geometries of the two tools were characterized by the AFM. After the cantilever tip radius was measured, scans of the flat-nosed tool edge cross-sections were made. Repeated measurements were made across the center 1 mm portion of the tool to confirm edge uniformity. The final characterization was based on three 2 µm x 2 µm scans of the tool edge, one along the tool centerline and one on each side, 150 µm from the center. Fig. 3 shows the measured profiles of the two tools after taking into account the measured cantilever tip radius of 35 nm. The edge of the new tool (Tool 1) was nearly a true radius of 75 nm ±15 nm. The worn tool (Tool 2) showed, at it sharpest point, an edge radius of approximately 105 nm, and a gradually changing flank face slope characteristic of previous measurements of tools with various degrees of wear (Asai et al., 1990; Horio et al., 1992; Lucca and Seo, 1993a). Fig. 4 shows the geometry of the tool edge represented by its curvature (the inverse of the local edge radius) plotted as a function of distance along the tool edge. This distance is measured from a line which bisects the rake and flank faces, and passes through the point of their intersection (the point at the tool edge for an infinitely sharp tool). Shown is the ideal case of a tool with a circular edge radius of 75 nm, along with the actual measured geometries of Tool 1 and Tool 2. We have defined the rake and flank faces from their theoretically sharp intersection point. The actual geometries show variation from a true circular edge by a rounding of the ideal profile. Tool 2 shows the effects of wear by a shifting upward along the rake face of the sharpest point, and a broadening along the flank face, responsible for the larger tool-workpiece contact for the worn tool. For comparison, the worn tool

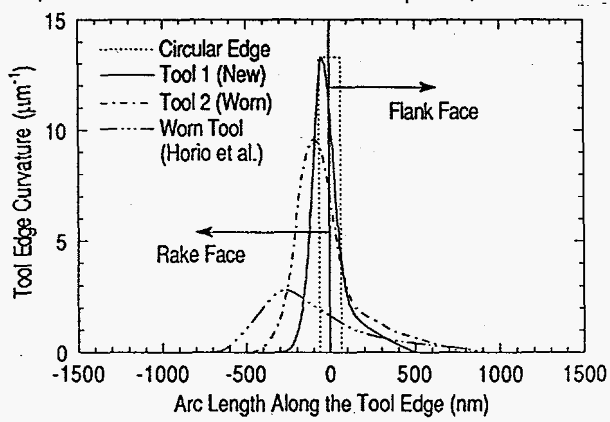

Fig. 4 Inverse of Local Edge Radius Measured Along the Tool Edge

geometry reported by Horio et al., (1992) is also shown.

The magnitudes of the cutting and thrust forces were obtained over the uncut chip thickness range of 0.01-10 µm by the average heights in the cyclic force signals. Figs. 5 and 6 show the cutting and thrust forces obtained for both tools when machining Te-Cu. Consistent with previous results, the new and worn tools, which have the same nominal geometry, are seen to yield the same forces at large uncut chip thicknesses (Lucca et al., 1991,1993a). The effects of the difference in their tool edge profiles are seen to a degree in the cutting force curve, and more so in the thrust force curve below several micrometers. The difference in the thrust forces of the two tools is consistent with the difference in their edge profiles. For example, an estimate of the contact length at the tool-workpiece interface using the measured thrust force at an uncut chip thickness of 0.2 µm, and assuming an interfacial pressure of 3 times the uniaxial yield strength of the workpiece material (225 MPa for Te-Cu), is 0.2 µm and 0.9 µm for Tools 1 and 2 respectively. From Fig. 3, examination of the lengths of their flank faces which would be in contact when cutting at this depth indicates very similar values.

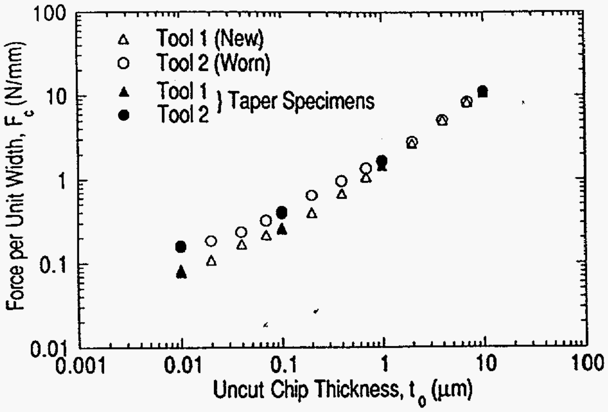

Fig. 5 Measured Cutting Force as a Function of Uncut Chip Thickness When Machining Te-Cu with Tool 1 and Tool 2

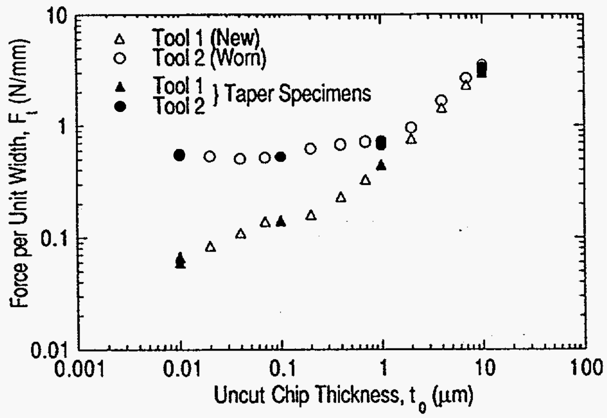

Fig. 6 Measured Thrust Force as a Function of Uncut Chip Thickness When Machining Te-Cu with Tool 1 and Tool 2

To arrive at a measure of the depth of the subsurface plastic deformation resultant from machining at a given uncut chip thickness, workpiece specimens were prepared for taper sectioning. Surfaces were machined at four uncut chip thicknesses, viz., 10, 1, 0.1, and 0.01 μm for both Te-Cu and fine grain Cu. Care was taken to ascertain that the surface generated was representative of cutting at the uncut chip thickness of interest by removing at least 50 μm of surface while machining at uncut chip thicknesses of 0.01 and 0.1 μm, and several hundred micrometers for uncut chip thicknesses of 1 and 10 μm. Figs. 5 and 6 show the force data obtained when cutting the four Te-Cu specimens overlaid on the data obtained for the complete range of uncut chip thickness. Force data was taken twice for each specimen. The specimens were then polished, the taper interface characterized, and the taper surface etched. The nominal taper angle was 5 degrees. Repeated polishing and etching was performed to yield a total of four readings of plastic layer thickness for each specimen. Changes in the interface geometry after re-polishing were measured and accounted for. After etching, the plastically deformed layer was revealed. Fig. 7 shows two etched surfaces with the zone of plastic deformation visible as the dark band at the taper interface. Fig. 7a) is the etched surface obtained for a Te-Cu specimen which was machined at an uncut chip thickness of 1.0 μm with Tool 1, and Fig. 7b) shows the result for a fine grain Cu specimen machined at an uncut chip thickness of 0.01 μm with Tool 2. The dark-etched "outer fragmented layer" as it is referred to by Samuels (1971) is clearly visible as well as the zones of less strained regions. No attempt was made to obtain a quantitative measure of the percent strain which the darkened region in the present study represents, although studies correlating shading with precise measures of percent compression strain have been reported for Cu and alpha-brasses (Samuels, 1954). Some darker shading in the bulk regions for both the Te-Cu and fine grain Cu (lower portion of Figs. 7a) and 7b)) can be seen, and may be an indication of remaining subsurface plastic deformation created during the mechanical polishing of the specimen. This shading was seen to diminish with longer etching time, although increasing the etching time involved pitting of individual grains. Although the clarity of the plastically deformed layer at the diamond-cut surface varied with etching time, the overall region developed quickly and did not change dimension. Fig. 7a) also shows some remnant polishing marks in the subsurface, and Te droplets in the bulk material (elongated in some cases) are clearly visible. The upper portions of Figs. 7a) and 7b) are views of the diamond-cut surface seen through the clear mounting plastic. Fig. 7a) shows the grain relief structure which is generated when diamond cutting at relatively large uncut chip thicknesses, and diamond knife (edge) marks are seen in Fig. 7b) characteristic of the burnished surface created at small uncut chip thicknesses (Moriwaki, 1989).

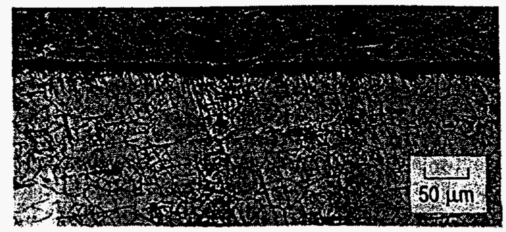

a) Te-Cu Machined with Tool 1, Uncut Chip Thickness = 1.0 μm

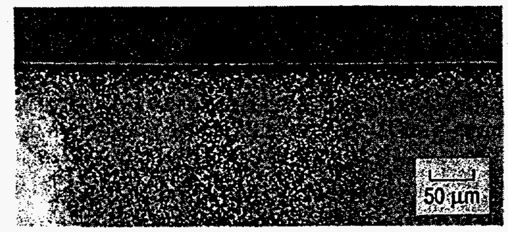

b) Fine Grain Cu Machined with Tool 2, Uncut Chip Thickness = 0.01 μm

Fig. 7 Etched Taper Specimens Revealing Depth of Subsurface Plastic Deformation

The results obtained for the depth of the plastically deformed layer when machining Te-Cu with Tools 1 and 2 are shown in Fig. 8. The fine grain Cu results were found to be very similar. Whereas the difference in edge geometries of the two tools resulted in a significant difference in their measured thrust forces at low uncut chip thickness, this difference was not observed in the measured depth of the plastic layer. Also, depth of the plastic layer was uncorrelated with uncut chip thickness. This is consistent with the results of Carr et al. (1991) for the three dimensional diamond flycutting of single crystal Cu. Shown also in Fig. 8 is an estimate of the elasto-plastic boundary beneath the surface which was made by considering the elastic solution of an inclined line load acting at the surface of a semi-infinite solid using the measured force components. The components for normal and shear stress beneath the surface can be written as:

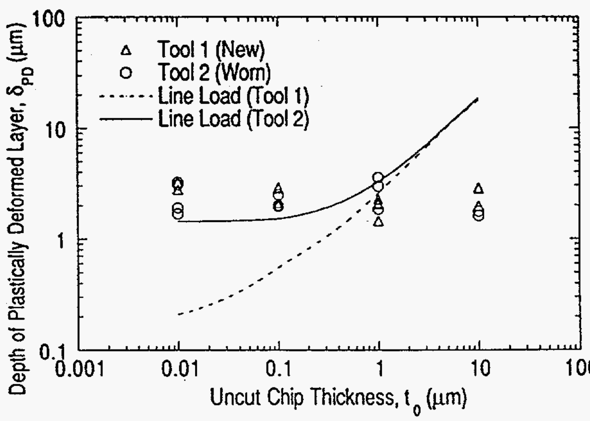

Fig. 8 Measured Depth of Subsurface Plastically Deformed Layer for Machining Te-Cu Along with Results Calculated for a Line Load on a Semi-Infinite Solid

$$\sigma_{xx} = \beta x^2,\ \sigma_{yy} = \beta y^2,\ \sigma_{xy} = \beta xy$$

$$\text{where } \beta = \frac{2F_t}{\pi}\left(\frac{F_c}{F_t}x - y\right)\frac{1}{\{x^2+y^2\}^2}$$

where F_c is the cutting force and F_t is the thrust force. The surface is defined by y=0, and F_c acts in the -x direction. By locating the depth at which the equivalent von Mises stress is equal to the plane strain yield strength of the workpiece material, an estimate of the plastically deformed layer thickness was made. This depth, predicted by a more complete elasto-plastic analysis, was seen to be in reasonable agreement with the elastic solution. The solution should be most applicable when the measured forces indicate sliding-indentation (as opposed to cutting) to be dominant (Lucca et al., 1993b), i.e., when $F_t/F_c > 1$. From Figs. 5 and 6 this is seen to be the case when machining with Tool 2 at low uncut chip thickness. The measured plastic layer depths show reasonable agreement with the line load solution for this case. The two-dimensional model of surface generation in ultraprecision machining of Ikawa and Shimada (1977) can also be used to obtain an estimate of the depth of the plastic layer. Plastic flow at the tool edge was modeled as the elasto-plastic deformation of a thick-walled tube subjected to an internal pressure. Their result is solely (and linearly) dependent on the edge radius of the tool when assuming an indentation pressure equal to three times the uniaxial yield strength of the workpiece material. For an edge radius of 75 nm, their result yields a plastic layer thickness of 0.9 µm.

Several experimental investigations have reported on the depth of the plastically deformed layer when diamond flycutting in a facing, or three dimensional, configuration. Horio et al. (1992) determined the depth of the plastically deformed layer by residual stress measurements when diamond flycutting an Al-Mg alloy. For a nominal depth of cut of 5 µm, depths of approximately 1.8 and 17 µm were reported for a new and worn tool respectively. Their new tool was characterized as having an edge radius of 50 nm, while the worn tool had a edge radius at the rake face of 350 nm. In view of the differences with the present study in workpiece material and edge geometries (Fig. 4 shows that Tool 2 of the present study was substantially sharper), any direct comparisons must be made with caution. Carr et al. (1991) has reported on the depth of subsurface damage for various crystal orientations of Cu observed by TEM. It was found that depth of damage was unaffected by cutting velocity, feed rate and nominal depth of cut over the range of 0.3-6 µm. Crystal orientation was seen to have the largest effect, and depths of damage observed were 4.4, 3.4, and 2.3 µm when machining the {100}, {110} and {111} surfaces respectively. In the present experiments, the variation of observed plastic depth as a result of the crystallographic orientation of the Te-Cu grains at the machined surface was clearly seen. The overall magnitudes of the measured depths in the present study appear to be consistent with these results.

5. CONCLUSIONS

The depth of the plastically deformed layer at the workpiece surface which results in the orthogonal ultraprecision machining of Cu over the range of uncut chip thicknesses of 0.01-10 µm was investigated. Two tools with the same nominal geometry but with differing edge geometries were used to machine both Te-Cu and fine grain Cu. Tool edge geometries were characterized by atomic force microscopy, taking into account the AFM cantilever tip radius. Whereas the two tools exhibited substantially differing force behavior with uncut chip thickness below several micrometers, this behavior was not observed for the measured depth of the plastically deformed layer. In addition, the depth of plastic layer appeared unaffected by the uncut chip thickness. Magnitudes of the measured depths appear to be consistent with values reported in the literature and those arrived at by simple analyses.

ACKNOWLEDGEMENTS

The authors would like to thank Dr. R.R. Donaldson for his many valuable suggestions in this study, in particular his significant guidance on the characterization of the diamond tools. Also, we would like to thank Drs. M.F. DeVries, R.J. Hocken, and R. Komanduri for their valuable suggestions and comments, and Dr. W. Siekhaus for advice regarding the microsphere calibrations. The kind support by the National Science Foundation, Division of Design and Manufacturing Systems through Grant No. DDM-9215613 is gratefully acknowledged. We extend thanks to Dr. B.M. Kramer for his interest, encouragement and support. Funding provided by the Oklahoma Center for the Advancement of Science and Technology, and the Department of Energy is also gratefully acknowledged.

REFERENCES

(1) Asai, S., Taguchi, Y., Horio, K., Kasai, K., Kobayashi, A., 1990, Measuring the Very Small Cutting-Edge Radius for a Diamond Tool Using a New Kind of SEM Having Two Detectors, Annals of the CIRP, 39, 1: 85-88.

(2) Carr, J. W., Narayan, C., Kim, J., 1991, Single Point Diamond Machining Induced Damage on Single Crystal Copper, Aluminum and Gold, Proceedings, ASPE Annual Meeting, 96-99.

(3) Dautzenberg, J. H., van Dijck, J. A. B., Kals, J. A. G., 1989, Metal Structures by Friction in Mechanical Working Processes, Annals of the CIRP, 38, 1: 567-570.

(4) Evans, C., Polvani, R., Postek, M., Rhorer, R., 1987, Some Observations on Tool Sharpness and Sub-Surface Damage in Single Point Diamond Turning, SPIE, In-Process Optical Metrology for Precision Machining, 802, 52-66.

(5) Hahn, R. S., 1963, On the Nature of the Grinding Process, Advances in Machine Tool Design and Research, A Pergamon Press Book, The Macmillan Company, Proc. 3rd Int. M.T.D.R. Conf., 129-154.

(6) Horio, K., Kasai, T., Ogata, Y., Kobayashi, A., 1992, A Study on Damaged Layer Remaining in Diamond Mirror Cut Surface, Annals of the CIRP, 41, 1: 137-140.

(7) Ikawa, N., Shimada, S., 1977, Cutting Tool for Ultraprecision Machining, Proc. of the 3rd Int. Conf. on Production Engineering, Tokyo, 357-364.

(8) Lucca, D. A., Rhorer, R. L., Komanduri, R., 1991, Energy Dissipation in the Ultraprecision Machining of Copper, Annals of the CIRP, 40, 1: 69-72.

(9) Lucca, D. A., Seo, Y. W., 1993a, Effect of Tool Edge Geometry on Energy Dissipation in Ultraprecision Machining, Annals of the CIRP, 42, 1: 83-86.

(10) Lucca, D. A., Seo, Y. W., Rhorer, R. L., 1993b, Energy Dissipation in Ultra-Precision Machining, Proceedings of the 1993 NSF Design and Manufacturing Systems Conference, 1, 225-229.

(11) Moriwaki, T., Okuda, K., 1989, Machinability of Copper in Ultra-Precision Micro Diamond Cutting, Annals of the CIRP, 38, 1: 115-118.

(12) Nakayama, K., Tamura, K., 1968, Size Effect in Metal-Cutting Force, Trans. ASME, J. Eng. Ind., Feb., 119-126.

(13) Rigney, D. A., Hirth, J. P., 1979, Plastic Deformation and Sliding Friction of Metals, Wear, 53, 345-370.

(14) Samuels, L. E., 1954, The Metallographic Detection of Deformation in Copper and Alpha-Brasses, J. the Institute of Metals, 83, 359-368.

(15) Samuels, L. E., (2ed.), 1971, Metallographic Polishing by Mechanical Methods, American Elsevier Publishing Co., Inc., New York.

(16) Sugano, T., Takeuchi, K., Yoshida, Y., 1987, Diamond Turning of an Aluminum Alloy for Mirror, Annals of the CIRP, 36, 1: 17-20.

(17) Suh, N. P., 1986, Tribophysics, Prentice-Hall, Inc., Englewood Cliffs, New Jersey.

(18) Turley, D. M., Samuels, L. E., 1981, The Nature of Mechanically Polished Surfaces of Copper, Metallography, 14, 275-294.

(19) von Turkovich, B. F., 1972, On a Class of Thermo-Mechanical Processes During Rapid Plastic Deformation (with Special Reference to Metal Cutting), Annals of the CIRP, 21, 1: 15-18.